Mechanism of the Membrane Potential Sensitivity of the Fluorescent Membrane Probe Merocyanine 540†

Paul R. Dragsten‡ and Watt W. Webb*

ABSTRACT: The fluorescence and optical absorption of the membrane-staining dye merocyanine 540 (M-540) have been widely used to measure cellular transmembrane potentials. We have studied the molecular mechanisms of these optical changes by measuring the fluorescence polarization of M-540 and its response to membrane potential changes in hemispherical lipid bilayer membranes. The fluorescence responds to a potential step in two distinct time scales: a fast response with a rise time less than the instrumental capability of 6 μs and a slow response with a time constant around 10^{-1} s. Both response amplitudes are proportional to the amplitude of the membrane potential change and both require an asymmetrical distribution of M-540 across the membrane. The slow response is ascribed to a net change of the dye concentration in the membrane. The fast response appears to be dominated by a change in the distribution of orientations of the dye molecules in the membrane, with a concomitant perturbation of a monomer–dimer equilibrium, due to interaction of the applied electric field with the permanent molecular dipole moment of M-540. The amplitude of the fast fluorescence response is concentration dependent and can be modeled by including membrane saturation effects and the presence of a nonfluorescent dimer species in the membrane at high dye concentrations. Absorbance changes reported by other investigators are consistent with this model mechanism.

Until the recent development of optical probes of membrane potential, measurements of cell membrane potentials were restricted to cells large enough to be impaled safely with a microelectrode. In 1968, Tasaki et al. (1968) demonstrated that nerve activity could be detected by monitoring changes in the fluorescence emitted by neurons stained with 1-anilinonaphthalene-8-sulfonate (1,8-ANS). Since then, several hundred dyes have been tested as membrane potential probes (Cohen et al., 1974; Ross et al., 1977), and fluorescence and absorption changes have been used to monitor membrane potentials in phospholipid vesicles and cell suspensions (Sims et al., 1974), nerve membranes (Cohen et al., 1974; Tasaki et al., 1973), and heart and skeletal muscle systems (Carnay and Barry, 1969; Landowne, 1974; Oetliker et al., 1975; Salama and Morad, 1976; Vergara and Bezanilla, 1976). The dye merocyanine 540 (M-540)[1] and some of its analogues in particular were found to give some of the largest fluorescence and absorption signals on the time scale of a nerve action potential. Fluorescence intensity changes of about one part in 10^3 and absorbance changes of $\sim 10^{-4}$ were observed to accompany action-potential pulses in axon preparations (Davila et al., 1973; Salzberg et al., 1973; Cohen et al., 1974; Ross et al., 1974a,b).

We report here our investigation of the mechanism of the fluorescence response of M-540 to membrane potential changes. Previous ideas about the mechanism of this response are based on measurements of the spectral dependence of the amplitudes of fluorescence intensity and optical absorption changes in externally stained axons. Fluorescence measurements have shown transient increases in intensity during axon depolarization, with an action spectrum the same shape as the static fluorescence excitation spectrum. Absorbance changes, on the other hand, are positive (increase in axon absorption upon depolarization) for wavelengths between 550 and 620 nm and negative between 460 and 550 nm. These results have been attributed to transient conversion of a nonfluorescent dimer species on the membrane into fluorescent monomers during membrane depolarization (Ross et al., 1974a,b; Tasaki et al., 1976; Waggoner, 1976; Waggoner and Grinvald, 1977). Some cyanine dyes are known to form nonfluorescent dimers with absorption maxima shifted toward shorter wavelengths (Sims et al., 1974; West and Pearce, 1965). However, Tasaki and Warashina (1976) have also shown that signals from absorption of polarized light are consistent with a simultaneous spectral shift and orientation change of the dye during action potentials.

Since molecular reorientation of the dye in the large electric fields in the lipid membrane might be involved in the fluorescence response, we performed fluorescence polarization measurements on single, oriented bilayer membranes labeled with M-540. Such measurements have previously been useful in determining fluorophore alignments in membrane and liquid crystal systems (Yguerabide and Stryer, 1971; Badley et al., 1971, 1972, 1973; Tasaki et al., 1973; Carbone et al., 1975; Frehland and Trissl, 1975). We measured the transient changes in the polarized fluorescence intensities induced by voltage pulses applied across the membrane using a voltage clamp system. Steady-state fluorescence polarization measurements provided a measure of the equilibrium distribution of orientations. To discriminate amongst various possible response mechanisms, we investigated the effects of dye concentration, excitation and emission spectra, and the time scales of the fluorescence changes.

Materials and Methods

Cholesterol, obtained from Sigma Chemical Co. (St. Louis), was oxidized by boiling in octane according to the procedure of Tien (1974). The octane was evaporated and the oxidized cholesterol redissolved in decane prior to each experiment. Decane (spectral grade) was obtained from Aldrich Chemical

† From the Physics Department (P.R.D.) and School of Applied and Engineering Physics (W.W.W.), Cornell University, Ithaca, New York 14855. This work was supported by grants from the National Science Foundation and benefited from facilities of the Materials Science Center at Cornell.

‡ Present address: Laboratory of Theoretical Biology, National Institutes of Health, Bethesda, Md. 20014.

[1] Abbreviations used: M-540, merocyanine 540; FCS, fluorescence correlation spectroscopy.

0006-2960/78/0417-5228$01.00/0

Co. (Milwaukee) and merocyanine 540 from Eastman Kodak Co. (Rochester, N.Y.)

Membrane Formation. Bilayer lipid membranes were formed from a solution of oxidized cholesterol in decane (30 mg/mL) on the fire-polished tip of a pasteur pipet which had been treated with silane surfactant (Z-6076 or XZ2-2024, Dow Chemical Co.). The pipet was filled with a solution of 0.05 M sodium phosphate buffer (pH 7.0) and 0.05 M NaCl, the very tip was filled with membrane-forming solution, and the pipet was lowered into a cuvette of the same buffer solution which also contained the M-540 and 0.5% (v/v) ethanol as a dispersant. A hemispherical bilayer was then formed by depressing a micrometer-driven syringe in the top of the pipet and allowing the lipid bubble thus formed to thin to bilayer thickness.

Membrane Potential. Voltage pulses were applied across the membrane by a voltage clamp circuit employing two pairs of electrodes: a Pt-black pair for passing current and an Ag-AgCl pair for monitoring voltage. The time constant for applying a step change in membrane voltage, which was limited by the membrane capacitance and series resistance of the aqueous solution, was about 0.5 ms. In experiments attempting to measure faster fluorescence response times, this time constant was reduced to between 2 and 6 μs by increasing the salt concentration to 0.5 M, increasing the pipet diameter, decreasing membrane capacitance by bulging the membrane only slightly, and adding a compensating capacitive lag to the voltage-measuring circuitry (for details, see Dragsten, 1977).

Fluorescence. Membrane fluorescence was excited by intersecting the membrane with a focused laser beam (at 70-μW power) at one of the three points shown in Figure 2. Excitation at 514.5 nm was obtained from either a Coherent Radiation Model CR3 or a Spectra Physics Model 164-03 argon ion laser, and excitation between 575 and 600 nm from an argon ion laser-pumped dye laser (Coherent Radiation Model 490) using Rhodamine 6G. A half-wave plate linear polarizer combination was used to rotate the plane of polarization of the excitation beam. Fluorescence was collected with an objective lens of 6.3× magnification and 0.12 numerical aperture (which introduces only a negligible correction to the polarization measurement (Dragsten, 1977)), passed through a Corning short-wavelength cutoff filter and an analyzer polarizer, and detected with a cooled RCA 7265 photomultiplier. The observed area of the membrane was limited by an aperture placed in the image plane of the objective and could be viewed directly with a retractable 45° mirror-telescope combination. The membrane was essentially planar over this viewed area. The photomultiplier output was analyzed with a Northern Scientific Model 575 signal averager which was preceded by a Biomation Model 8100 transient recorder for short time-constant measurements. The response time of the light-measuring system was 2 μs. All fluorescence measurements were corrected for laser intensity variations and solution absorption, and the contribution of the aqueous solution fluorescence was subtracted.

Experiments were carried out at room temperature, except for some observations of the fast time constant, which were done at 5 ± 1 °C. In this last case, a cylindrical copper enclosure containing the sample cuvette was cooled and temperature controlled by a circulating water bath.

Diffusion Coefficient and Concentration Measurements. Measurements of the dye concentration in the membrane and diffusion constant in aqueous solution were made utilizing the technique of fluorescence correlation spectroscopy (FCS) (Magde et al., 1972, 1974; Elson and Magde, 1974; Koppel et al., 1976; Fahey et al., 1976). In this technique, the amplitude and time correlations of fluctuations in the fluorescence intensity from a small illuminated volume are analyzed to determine both the average number of molecules in the illuminated volume and the characteristic time a molecule spends in the volume. This permits the calculation of the average concentration of independent fluorescence particles and their diffusion coefficient. In membrane experiments, the laser beam was focused down to a small spot (~1.2-μm radius) on the membrane, and in the free-solution experiments the illuminated volume was defined by the intersection of the focused laser beam with a 50-μm thick rectangular capillary filled with the dye solution.

Results and Discussion

The sensitivity of the fluorescence of membrane-bound M-540 to membrane potential was characterized by measuring membrane fluorescence with various concentrations of M-540 added to the aqueous phase on one side of the membrane. We measured the steady-state fluorescence intensity and polarization and the transient response following step changes of membrane potential. Aspects of the excitation and emission spectra were also studied.

To describe the results efficiently, we first outline a notation for the optical geometry of the polarization experiments. Second, we outline some suggested mechanisms to indicate the rationale of our analysis. Third, we present and analyze qualitatively the results of the experiments outlined above. Finally, we discuss several conclusions deduced from these experiments. The first of these is a quantitative model for the important fast fluorescence response; the second is an application of our results to the understanding of fluorescence changes observed in a cylindrical membrane geometry, such as on a nerve axon. In conclusion, we present a summary of our essential findings.

Fluorescence Polarization Notation. Using the optical geometry of Figure 2 with the three beam positions shown, it is possible to measure fluorescence intensities from all possible combinations of orthogonal orientations of excitation polarization, emission polarization, and plane of the membrane. This result is illustrated in Figure 3, where our notation for the various fluorescence polarizations is introduced. The static fluorescence intensities are denoted I_{ij}, where i is the excitation polarization direction and j the emission polarization direction relative to the set of coordinate axes fixed in the membrane. Similarly, the symbols Δ_{ij} denote the fractional change in intensity of I_{ij} when the potential of the inside compartment of the bubble membrane is brought to +100 mV from 0 V with respect to the outer compartment, and the dye is present in the outer compartment. "Membrane potential", henceforth, refers to the potential inside the bubble relative to the potential of the outer compartment. In the present study, fluorescence responses in two separate time ranges will need to be distinguished: a superscript s (Δ_{ij}^{s}) will refer to "slow" responses on a millisecond or longer time scale, and a superscript f (Δ_{ij}^{f}) to "fast" responses on a microsecond or faster time scale.

Since the 3 direction is taken normal to the membrane, the 1 and 2 directions in the membrane are equivalent; hence, $I_{13} = I_{23}$, $I_{31} = I_{32}$, $I_{11} = I_{22}$, and $I_{21} = I_{12}$. Similar considerations hold for the Δ_{ij}. In general, $I_{ij} \neq I_{ji}$ (except for I_{12}) if the angular distribution of molecular orientations with respect to membrane normal is not uniform over 4π sr and either (a) the emission and excitation dipoles of the dye molecule are nonparallel or (b) there is only limited reorientation during the molecule's excited-state lifetime (Badley et al., 1971). Thus, there remain in general five independent polarizations; in terms of the I_{ij} these are I_{11}, I_{12}, I_{13}, I_{31}, and I_{33}. Of these, I_{12} (or

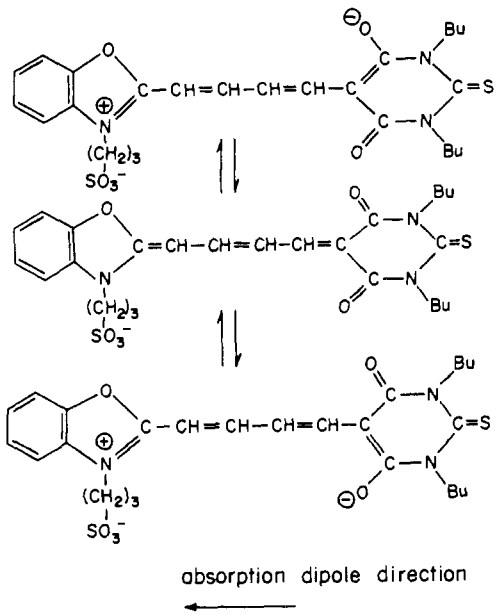

FIGURE 1: Molecular structure of M-540 including the resonant structures which contribute to the ground-state permanent dipole moment. Arrow shows assumed direction of the absorption dipole: M_r = 570; Bu = butyl.

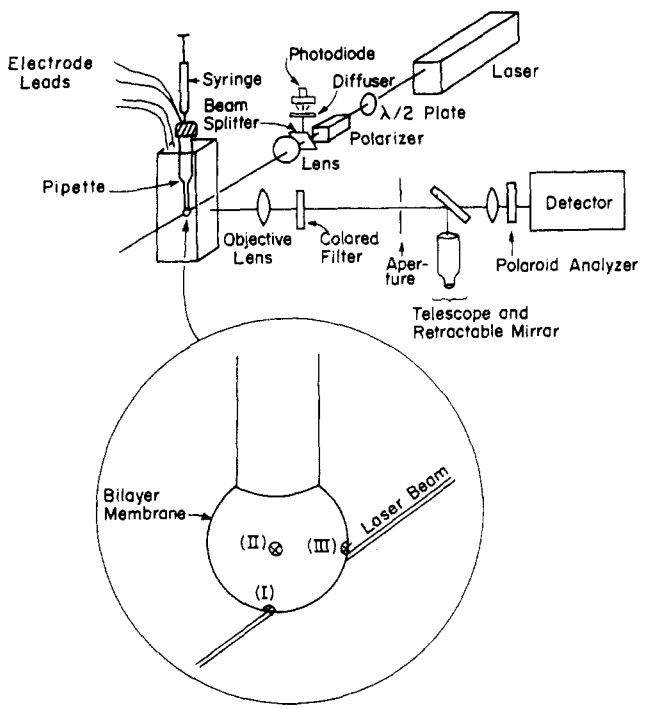

FIGURE 2: Diagram of the optical apparatus. The magnified inset shows the three points of intersection of the laser beam and membrane used in the experiments. The polarizer and analyzer were each used in two positions: to pass light with the electric vector polarized in either the horizontal or vertical direction. The beam monitor unit (photodiode, diffuser, and beam splitter) rotates with the polarizer so that the beam splitter reflects light polarized in the plane of incidence regardless of the polarizer orientation.

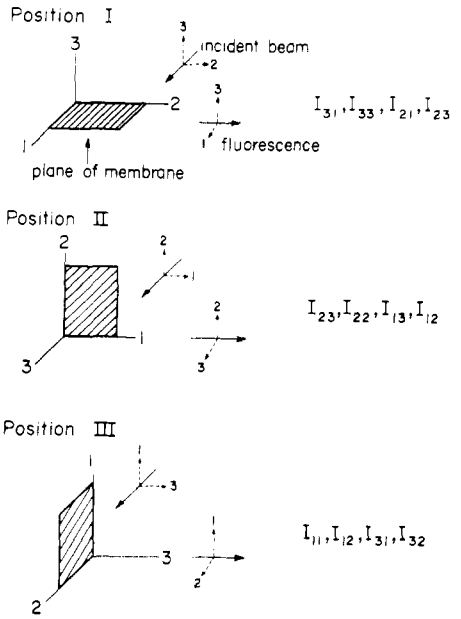

FIGURE 3: Fluorescence polarization geometry showing the possible polarization directions of the incident excitation light and collected fluorescence and the orientation of the membrane relative to the specified set of coordinate axes. The dotted arrows show the alternative polarization directions for the incident excitation light and collected fluorescence electric vectors. The intersection point of the laser beam and membrane bubble corresponding to each position is shown in Figure 2, and the fluorescence polarization intensities measurable in each position are listed. Thus, I_{ij} denotes the fluorescence intensity for incident polarization i and fluorescence polarization j. Note that the membrane plane is always perpendicular to the 3 axis.

equivalently I_{21}) can be measured in all three membrane geometries (see Figure 3); hence, it was used to normalize the other I_{ij}, thereby correcting for the possibility of observing different membrane areas in different orientations. The measured values of I_{12}, and thus the normalization factors, varied at most by a factor of 2, and typically no more than 40%, between positions. Values of I_{ij} subsequently reported have been thus normalized.

A fluorescent molecule preferentially absorbs and emits light polarized parallel to the orientation of its absorption and emission dipoles, respectively. In the case of M-540, the emission dipole is nearly parallel to the absorption dipole (Dragsten, 1977). (See Figure 1 for the direction of the absorption dipole.) Thus, I_{11} and I_{12} and the corresponding Δ_{11} and Δ_{12} reflect the component of molecular orientations parallel to the plane of the membrane. Similarly, I_{33} and Δ_{33} preferentially sample the perpendicular orientation.

It is also useful to define the quantities $\alpha_i = \Sigma_{j=1}^{3} I_{ij}$, which are proportional to the total fluorescence excited by a beam of polarization denoted by the subscript i. If the absorption coefficient and fluorescence quantum efficiency of the dye are independent of the molecular orientation in the membrane, the relative magnitudes of the α_i are proportional to the relative magnitudes of the polarized absorption coefficients for the corresponding polarization directions, regardless of the degree of molecular reorientation during the excited-state lifetime.

Possible Mechanisms. Before presenting our experimental results, it will be useful to describe several mechanisms that have previously been considered as possibilities to account for fluorescence changes with potential.

(1) The partition coefficient of the dye between the membrane and aqueous phase may depend on membrane potential, thereby altering the membrane dye concentration and, consequently, the fluorescence intensity. The fractional fluorescence change (Δ_{ij}) due to this effect should show no polarization dependence and should decrease if the membrane becomes saturated with dye at high concentrations. It will be seen below that a slow response occurring with a time constant of a fraction of a second is most likely due to this mechanism (Dragsten and Webb, 1977).

TABLE I: Static Fluorescence Polarization Intensities.[a]

M-540 concn (μg/mL)	I_{11}	I_{12}	I_{33}	I_{13}	I_{31}	α_1	α_3
5	6.5×10^{-8} ($\pm$1.1)	3.1×10^{-8} ($\pm$0.5)	1.2×10^{-7} ($\pm$0.1)	5.0×10^{-8} ($\pm$0.5)	5.0×10^{-8} ($\pm$0.4)	1.5×10^{-7} ($\pm$0.1)	2.2×10^{-7} ($\pm$0.2)
2	5.6×10^{-8} ($\pm$0.4)	3.6×10^{-8} ($\pm$0.8)	1.3×10^{-7} ($\pm$0.1)	5.0×10^{-8} ($\pm$0.8)	6.1×10^{-8} ($\pm$0.6)	1.4×10^{-7} ($\pm$0.1)	2.5×10^{-7} ($\pm$0.2)
1	4.5×10^{-8} ($\pm$0.9)	3.0×10^{-8} ($\pm$0.7)	7.9×10^{-8} ($\pm$0.2)	4.0×10^{-8} ($\pm$0.7)	2.8×10^{-8} ($\pm$0.9)	1.2×10^{-7} ($\pm$0.1)	1.3×10^{-7} ($\pm$0.2)
0.5	3.2×10^{-8} ($\pm$0.2)	1.5×10^{-8} ($\pm$0.2)	3.4×10^{-8} ($\pm$0.4)	2.0×10^{-8} ($\pm$0.2)	8.9×10^{-9} ($\pm$0.8)	6.7×10^{-8} ($\pm$0.3)	5.2×10^{-8} ($\pm$0.4)
0.2	9.6×10^{-9} ($\pm$0.4)	2.6×10^{-9} ($\pm$0.1)	9.3×10^{-9} ($\pm$1.4)	4.8×10^{-9} ($\pm$0.8)	2.3×10^{-9} ($\pm$0.4)	1.7×10^{-8} ($\pm$0.1)	1.4×10^{-8} ($\pm$0.2)
0.1	4.4×10^{-9} ($\pm$0.6)	2.3×10^{-9} ($\pm$0.8)	4.2×10^{-9} ($\pm$0.6)	2.8×10^{-9} ($\pm$0.4)	1.1×10^{-9} ($\pm$0.2)	9.4×10^{-9} ($\pm$1.0)	6.5×10^{-9} ($\pm$0.6)
0.05	3.3×10^{-9} ($\pm$0.6)	1.1×10^{-9} ($\pm$0.1)	3.5×10^{-9} ($\pm$1.0)	1.2×10^{-9} ($\pm$0.2)	1.0×10^{-9} ($\pm$0.2)	5.5×10^{-9} ($\pm$0.6)	5.5×10^{-9} ($\pm$1.1)
0.01	9.7×10^{-10} ($\pm$1.3)	2.2×10^{-10} ($\pm$1.0)	8.0×10^{-10} ($\pm$1.6)	3.8×10^{-10} ($\pm$1.6)	3.7×10^{-10} ($\pm$1.4)	1.6×10^{-9} ($\pm$0.2)	1.5×10^{-9} ($\pm$0.3)

[a] The fluorescence intensities are given in terms of the detected fluorescence photocurrent. Each table entry is the average ($\pm$ the standard deviation) of between 8 and 40 individual fluorescence measurements.

(2) The orientation of the dye molecules in the membrane may depend on membrane potential. In this case, fluorescence intensity changes of both signs will be present among the various polarizations for a given membrane potential change, but there should be no total intensity change if all the fluorescence intensity changes are summed (i.e., $\Sigma_{i=1}^{3}\Sigma_{j=1}^{3}\Delta_{ij}I_{ij} = 0$). In axon experiments, the geometry is such that certain polarization components are weighted more heavily than others, so that complete cancellation would not occur. This mechanism is apparently responsible for a fast fluorescence response described below (Dragsten and Webb, 1977).

(3) The dye may change depth in the membrane (without an orientation change), thereby sampling a region of different polarizability. Since merocyanine 540 is very solvent sensitive (Brooker et al., 1965; Tasaki et al., 1976), its excitation or emission spectrum could be expected to shift in this case, thereby changing the detected fluorescence intensity. There should be little polarization dependence, but the fluorescence response should change sign as the excitation or emission wavelength is scanned.

(4) The dye's spectrum may shift due to an electrochromic effect (Bücher et al., 1969; Liptay, 1969; Platt, 1969). In this case, the sign of the fluorescence response would not change with polarization but the magnitude may. Again, the response should change sign as the excitation or emission wavelength is scanned, as with mechanism 3.

(5) The membrane potential may perturb the equilibrium constant for a membrane-bound monomer–dimer reaction in which the dimer is nonfluorescent, hence, changing the concentration of fluorescent monomers. Cyanine dyes in general are known to form nonfluorescent dimers (West and Pearce, 1965; Sims et al., 1974), and there is evidence of the presence of nonfluorescent M-540 dimers in membranes (Ross et al., 1974a,b; Warashina and Tasaki, 1975; Tasaki et al., 1976; Waggoner and Grinvald, 1977). Again, the sign of the fluorescence response should not change with polarization, and there should be a strong concentration dependence with the fluorescence response vanishing at low dye concentrations.

Fluorescence Polarization Measurements. The membrane was asymmetrically labeled with M-540 by introducing the dye (at various concentrations) into the aqueous phase outside the hemispherical membrane only. The dye quickly partitioned between the aqueous phase and the outer half of the lipid bilayer. That the dye does not redistribute equally between the two halves of the membrane is supported by three observations: (1) with the linear voltage dependence observed in the fast fluorescence response (see below), an equal concentration of dye on both sides of the membrane would give no voltage response, since the contributions from each side of the membrane would cancel; (2) neither the voltage-dependent signals nor aqueous solution fluorescence levels on either side of the membrane changed over a period of hours, indicating the dye distribution was stable; (3) adding M-540 to the aqueous solution inside the bubble gave fluorescence signals of opposite sign, which reversed upon subsequent addition of excess dye to the outer solution.

The steady-state polarized fluorescence intensities I_{ij} can be used to estimate molecular orientations in the membrane. The results of such measurements are listed in Table I along with the quantities α_1 and α_3 defined by $\alpha_i = \Sigma_{j=1}^{3}I_{ij}$. Judging from the α_i, molecular orientations neither perpendicular nor parallel to the membrane are strongly preferred. The fraction of the total fluorescence due to polarizations perpendicular to the membrane increases with increasing M-540 dye concentrations. Figure 4 also shows that the total fluorescence intensity ($\Sigma_{i=1}^{3}\Sigma_{j=1}^{3}I_{ij}$) saturates at high dye concentrations. This result suggests saturation of the membrane sites available to the dye.

More detailed insight into the equilibrium dye orientation distribution can be obtained by assuming particular model distributions (Dragsten, 1977). However, these calculations turned out not to be particularly valuable in elucidating the mechanism of potential sensitivity and are thus omitted.

When the membrane was asymmetrically labeled with M-540 as described above and rectangular voltage pulses were applied to the membrane, fluorescence changes in two distinct time ranges were observed. Figure 5 shows the fluorescence signal on a slow time scale. Notice that a fast fluorescence change is superimposed on a slow response with a time constant of a fraction of a second. Figure 6a shows that the fast response can be isolated using a faster time base. The fast response exhibits fluorescence changes of different signs for different polarizations; such a polarization dependence did not occur with the slow response. Since these fast and slow fluorescence

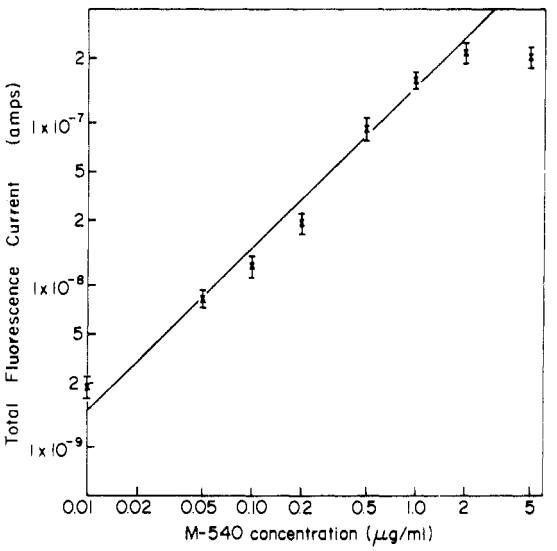

FIGURE 4: Summed photomultiplier current from all nine fluorescence polarizations $\Sigma_{i,j=1}^{3} I_{ij}$ as a function of the aqueous phase M-540 concentration. The fluorescence intensities and error bars, given in terms of the detected photocurrent, are calculated from Table I. The line slope is 1.

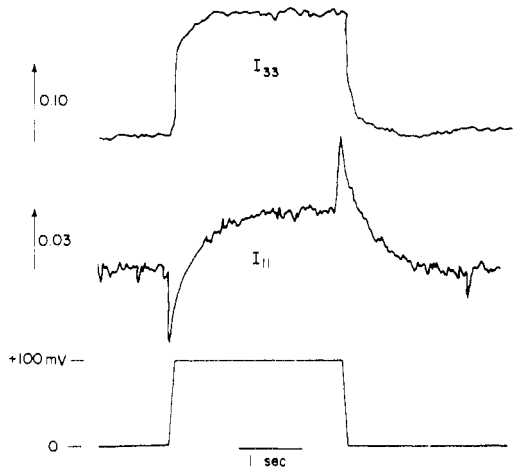

FIGURE 5: Fluorescence signals showing the slow response following the fast fluorescence response for a +100 mV membrane voltage pulse. The top trace (I_{33}) is averaged over 51 sweeps and the middle (I_{11}) over 198 sweeps. The bottom trace is the applied membrane potential. Solution concentration of M-540 is 0.5 μg/mL. The vertical arrows denote fractional fluorescence increases of the indicated magnitude.

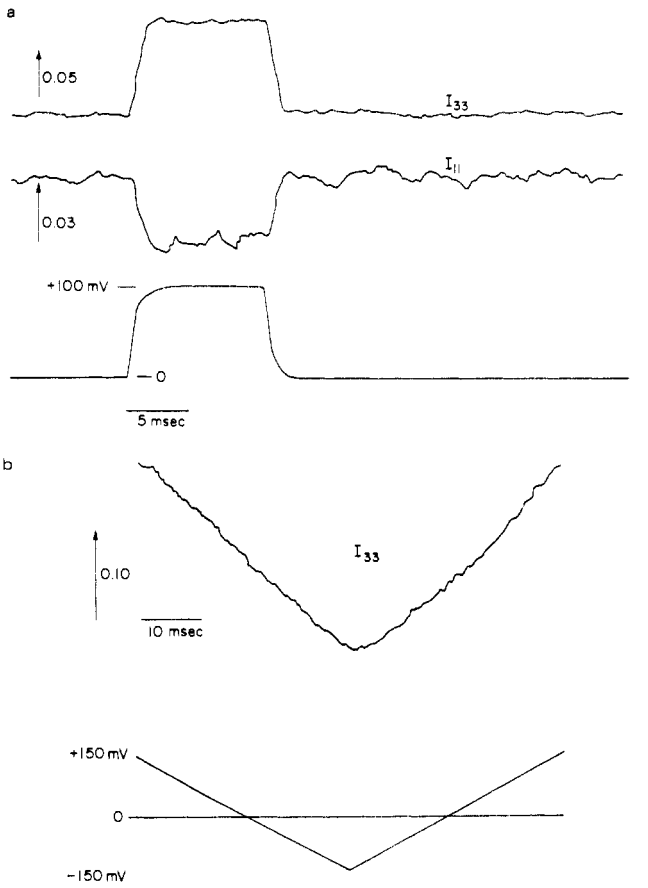

FIGURE 6: (a) Fast fluorescence response to a +100-mV membrane voltage pulse. The fluorescence signals (top two traces) were averaged 512 times. The applied voltage pulse (bottom trace) is recorded here with the same time constant as the fluorescence measuring system. Solution concentration of M-540 is 2.0 μg/mL. (b) Fast fluorescence signal (top trace) in response to potential ramp (bottom) demonstrating linearity with voltage. The fluorescence signal is averaged 70 times. Solution concentration of M-540 is 0.5 μg/mL. The vertical arrow indicates the scale of the fractional fluorescence increase.

responses can be clearly isolated, they will be considered separately below. A superscript s or f will be used to distinguish the slow and fast responses, respectively (Δ_{ij}^{s} and Δ_{ij}^{f}).

Slow Fluorescence Response. Within the reproducibility of the measurements, the fractional fluorescence changes in the slow response did not vary significantly with polarization. It is, therefore, sufficient to consider a simple average over the five independent fluorescence polarization responses. Figure 7 shows the average response $\Delta^{s} \equiv 0.2(\Delta_{11}^{s} + \Delta_{12}^{s} + \Delta_{13}^{s} + \Delta_{31}^{s} + \Delta_{33}^{s})$ as a function of the M-540 aqueous phase concentration. Subtractions of the contribution from the fast response were particularly difficult for polarizations where the fast and slow responses had the same sign (as in Figure 5, top trace) and were primarily responsible for the large uncertainties shown. In addition, fluorescent debris occasionally floated through the laser beam, adding to the noise in these slow time experiments. Nevertheless, Δ^{s} does decrease at the higher dye concentrations near the saturation level of the total membrane fluorescence ($\Sigma_{i=1}^{3}\Sigma_{j=1}^{3} I_{ij}$) seen in Figure 7. The sign of the slow fluorescence change is such that the fluorescence increases with membrane potential increases, that is, when the compartment *not* containing the dye is made positive. Reversal of the membrane potential reverses the sign of the fluorescence change. Since M-540 has a net negative charge at neutral pH, these results suggest that more dye is simply being electrochemically attracted to the membrane by positive membrane potentials.

Since the above evidence is all suggestive of mechanism 1 for the slow response, as a further test the time constants of the slow fluorescence changes were measured and compared with the time constants calculated for the response to an instantaneous change of the partition coefficient for the dye between the membrane and aqueous phase. The measured time constants are shown in Figure 8 as a function of the aqueous phase M-540 concentration. Most measurements fell in the range 0.2–0.6 s, and there was no discernible dependence on M-540 concentration within the rather large error limits.

The theory for the response to an instantaneous change in the partition coefficient has been worked out by Conti et al. (1974), who showed that the fluorescence response should have the form $1 - \exp(Dt/K_a^2)\mathrm{erfc}(\sqrt{Dt}/K_a)$, where $\mathrm{erfc}(x) = 1 - (2/\pi^{1/2}) \int_0^x e^{-z^2} dz$, t is the time after the step change in the partition coefficient, D is the diffusion constant of the dye in

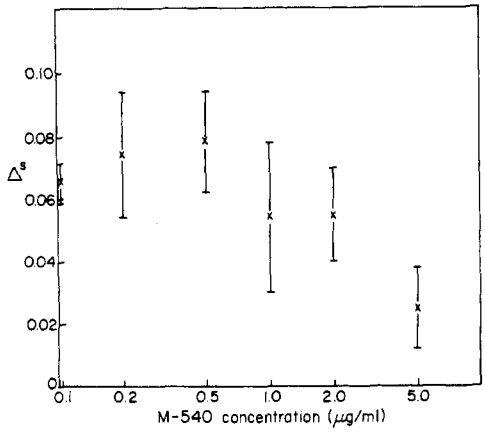

FIGURE 7: Slow fluorescence response: fractional change as a function of the aqueous phase M-540 concentration. $\Delta^s = (1/5)(\Delta_{11}{}^s + \Delta_{12}{}^s + \Delta_{13}{}^s + \Delta_{31}{}^s + \Delta_{33}{}^s)$ is an average over the five independent polarizations. The individual $\Delta_{ij}{}^s$ do not vary significantly among themselves relative to our experimental error. Each point represents an average of at least 32 individual measurements. The error bars are the standard deviations of the measurements.

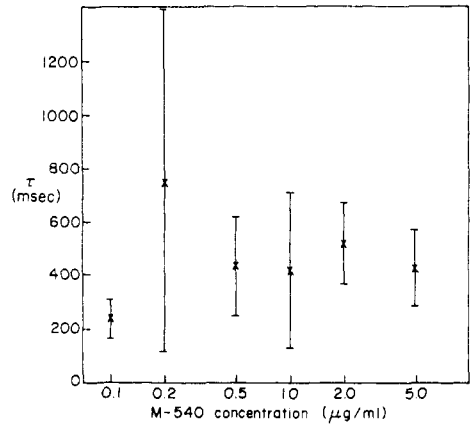

FIGURE 8: Time constant of the slow fluorescence response as a function of the aqueous phase M-540 concentration, assuming exponential decay. The time constants for all polarizations are averaged, with at least 20 measurements per point. Error bars are the standard deviations of the measurements. The large error bar at 0.2 μg/mL is the result of a bimodal distribution of data, with approximately half the measurements giving time constants between 0.2 and 0.4 s, and the other half between 1.0 and 1.5 s. The reason for this anomaly is unknown; we attribute it to a systematic artifact present in that particular measurement.

aqueous solution, and the adsorption constant K_a is the dye concentration on the membrane divided by the aqueous phase concentration. This theory assumes that the adsorption reaction at the membrane surface is very fast, so the rate-limiting step is diffusion to or from the membrane.

In order to calculate the time constant $K_a{}^2/D$, it is necessary to know both the bulk phase diffusion constant and the dye concentration on the membrane. Both these measurements were accomplished using the FCS technique described earlier (Dragsten, 1977). It was determined that, with an aqueous dye solution of 0.01 μg/mL (1.75×10^{-8} M), there were 160 molecules in the membrane in a circle of radius 1.2 μm. Since the molecular weight of M-540 is 570, $K_a = 3.4 \times 10^{-4}$ cm. In the aqueous phase, $D = 9.8 \times 10^{-7}$ cm^2 s^{-1} for a M-540 concentration of 0.027 μg/mL (4.7×10^{-8} M).

These values of K_a and D yield a calculated value of ~0.1 s for the time constant. This is less than our measured time constant, though of the same order of magnitude. For simplicity of analysis of our experimental data, we assumed an exponential decay instead of the functional form derived by Conti et al. (1974). The precision and reproducibility of our data were not sufficient to discriminate confidently between these two decay shapes. When we applied our mode of analysis to a curve calculated according to Conti's theory, we overestimated the decay time by as much as 70% due to the slowly decaying tail at long times (see Figure 8 of Conti et al., 1974). In addition, our measurement of D was necessarily performed at a lower dye concentration than was used in our determinations of the slow time constant. The propensity of M-540 for aggregation in solution (Tasaki et al., 1976) suggests that a smaller value for D, and hence a longer decay time $K_a{}^2/D$, may be appropriate for the higher dye concentrations used in our potential response experiments. In view of these facts, we think that the agreement is reasonable between the measured kinetics of the slow fluorescence change and the predicted response for diffusion-limited change of fluorophore concentration following a step change in partition coefficient.[2]

In summary, since the dye concentration dependence, kinetics, polarization properties, and sign of the fluorescence changes are all consistent with mechanism 1, we conclude that the slow fluorescence response is probably due to a voltage-induced change in the dye concentration on the membrane.

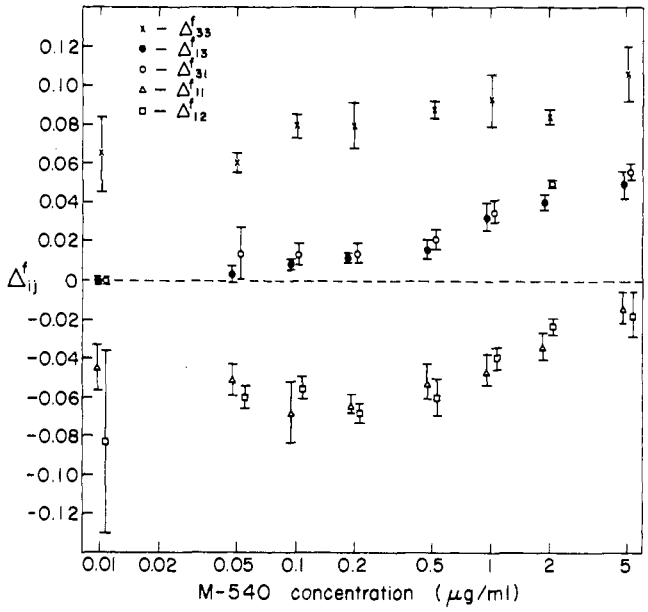

FIGURE 9: Fractional fluorescence changes for the fast response of the various fluorescence polarizations ($\Delta_{ij}{}^f$) as a function of the aqueous phase concentration. Error bars are standard deviations of the measurements.

Fast Fluorescence Response. As Figure 5 shows, a fast fluorescence change is always superimposed on the slow response discussed above. This fast response is undoubtedly responsible for the fluorescent detection of action potentials observed in experiments on nerve axons (Davila et al., 1973). The fast fluorescence response is linear with membrane voltage (Figure 6b); hence, an anisotropic dye distribution between the two sides of the membrane is essential.

Both the sign and amplitude of this response depend on the polarization. Figure 9 summarizes the data on the fast response as a function of the aqueous phase M-540 concentration. Two opposite trends are evident in the data: The positive fluores-

[2] Dye permeation through the membrane can in principle yield a similar slow relaxation of the fluorophore concentrations. However, the membrane permeability for M-540 is so small (Waggoner, 1976) that the associated relaxation times would be at least an order of magnitude larger than those observed.

cence responses (Δ_{33}^f, Δ_{13}^f, and Δ_{31}^f) all increase with increasing dye concentration, whereas the negative signals (Δ_{11}^f and Δ_{12}^f) decrease in magnitude with increasing concentration.

The fast response does *not* disappear at low concentrations, as expected of the voltage-dependent dimerization mechanism which has previously been invoked to explain absorbance changes (Ross et al., 1974a,b; Warashina and Tasaki, 1975; Tasaki et al., 1976). In this mechanism the dimer concentration would presumably vary quadratically with the monomer concentration at least at low M-540 concentrations and, therefore, should diminish rapidly as the dye concentration decreases.

An attempt was made to measure the time constant for the fast fluorescence response. Experiments performed at several M-540 concentrations between 0.05 and 1.0 μg/mL at room temperature and at 5 °C showed no fluorescence response slower than the 2 to 6 μs time required to apply a membrane voltage pulse. Cohen et al. (1974) reported measuring a time constant of 30 μs in a M-540-labeled squid axon at 13 °C.

These results can be compared to the rotational diffusion relaxation time for a prolate ellipsoid of approximately the dimensions of M-540. If τ_r is the rotational relaxation time about a minor axis of the ellipsoid, η the viscosity of the surrounding medium, and a and b the major and minor semiaxes, respectively, then from Tanford (1961)

$$\tau_r = 16\pi\eta a^3/3kT[-1 + 2\ln(2a/b)]$$

Using $a = 10$ Å, $b = 2$ Å, and $\eta = 1$–10 P [a typical range of viscosities found in membranes (Cogan et al., 1973; Shinitzky and Inbar, 1976)] we calculate $\tau_r \approx 0.1$–1 μs. Thus, the fluorescence response time would be too fast for us to detect. The slower response seen by Cohen et al. (1974) may be due to a higher effective viscosity of the squid axon membrane at 13 °C.

To detect the presence of a mechanism like 3 or 4, the fluorescence response was measured as a function of excitation wavelength and emission cutoff filter wavelength. No significant variations in Δ_{11}^f or Δ_{33}^f were found with cutoff filter half-transmission wavelengths between 522 and 625 nm or excitation wavelengths of 514.5, 576, 580, 590, or 600 nm. These results agree with Ross et al. (1974a) and Tasaki et al. (1976), who showed that the excitation spectrum of the fast fluorescence change has the same shape as the static fluorescence excitation spectrum and hence is not due to a spectral shift.

The results above provide quite compelling support for mechanism 2, voltage-induced molecular reorientation, as the dominant active process of the fast fluorescence response. The dependence of the signs of the fluorescence response on polarization can be explained only by this mechanism. The kinetics of this mechanism should be fast, as was observed, and the fractional fluorescence change should not depend on excitation or emission wavelength.

Furthermore, the signs of the fluorescence changes of the various polarizations are consistent with the molecular structure of M-540. The charged sulfonate group would not be expected to penetrate into the hydrophobic region of the membrane on energetic grounds. The energy required to move a group with a singe electronic charge e from a medium of dielectric constant ϵ_1 to a medium of dielectric constant ϵ_2 is

$$U = (e^2/2r)(1/\epsilon_2 - 1/\epsilon_1)$$

where r is the radius of the charged group. Using ϵ_1 (water) = 80, ϵ_2 (membrane) = 2, and $r = 3$ Å, U is calculated to be 1.9×10^{-12} erg (480 kcal/mol), an energy which yields the Boltzmann factor $\exp(-U/kT) \approx 10^{-20}$ at room temperature. Consequently, the SO_3^- group should remain at the aqueous interface and without penetrating significantly into the interior of the membrane. (This estimate neglects the relatively small effects of image charges and slow permeation which may introduce an additional very slow response.) Molecular reorientation then necessarily involves pivoting around the "anchored" sulfonate group. Application of an electric field applied to the membrane exerts a torque on the permanent dipole of the chromophoric region to reorient the molecule. From the molecular structure of Figure 1 it is apparent that a positive voltage applied to the inside of the bubble membrane should cause an increase in the polarized fluorescence intensities originating from molecular orientations perpendicular to the plane of the membrane (I_{33}). Likewise, fluorescence from parallel orientations (I_{11} and I_{12}) should decrease. Consequently, Δ_{33}^f should be positive and Δ_{11}^f and Δ_{12}^f negative, as is indeed observed (Figure 9).

The size of the effective molecular ground-state dipole moment that interacts with the applied electric field to produce the reorienting torque can also be estimated from our data by elementary consideration of a reorientation mechanism as follows: we define $\langle\mu_n\rangle$ and $\langle\mu_p\rangle$ as the average components of the ground-state dipole moment respectively normal and parallel to the plane of the membrane at zero potential and $\Delta\langle\mu_n\rangle$ and $\Delta\langle\mu_p\rangle$ as the changes associated with applications of a membrane potential V. The ratio of the changes of orientation induced by the membrane potential V can then be calculated from the Boltzmann distribution at thermodynamic equilibrium as

$$\frac{\langle\mu_p\rangle + \Delta\langle\mu_p\rangle}{\langle\mu_n\rangle + \Delta\langle\mu_n\rangle} = \frac{\langle\mu_p\rangle}{\langle\mu_n\rangle}\exp[-(\Delta E_p - \Delta E_n)/kT] \quad (1)$$

where k is the Boltzmann's constant, T is temperature, and ΔE_p and ΔE_n are the respective energy changes with voltage of a molecular dipole oriented parallel or normal to the membrane plane. If μ is the magnitude of the permanent molecular dipole moment, ϵ the dielectric constant in the membrane, and t its thickness, then $\Delta E_p = 0$ and $\Delta E_n = -\mu V/\epsilon t$. Equation 1 can be rewritten:

$$\frac{1 + \dfrac{\Delta\langle\mu_p\rangle}{\langle\mu_p\rangle}}{1 + \dfrac{\Delta\langle\mu_n\rangle}{\langle\mu_n\rangle}} = \exp[\mu V/(\epsilon t k T)] \quad (2)$$

With a ground-state dipole moment parallel to the molecular absorption dipole (as expected from Figure 1), $\Delta\langle\mu_p\rangle/\langle\mu_p\rangle = \Delta\alpha_1/\alpha_1$ and $\Delta\langle\mu_n\rangle/\langle\mu_n\rangle = \Delta\alpha_3/\alpha_3$, where, as defined above, α_i is the total fluorescence excited by "i" polarized light and $\Delta\alpha_i$ is the change with the voltage. Equation 2 then provides a formula for the molecular dipole in terms of the measured fluorescence changes:

$$\mu = \frac{\epsilon t k T}{V}\ln\left[\frac{1 + \Delta\alpha_1/\alpha_1}{1 + \Delta\alpha_3/\alpha_3}\right] \quad (3)$$

With $\epsilon = 2$, $t = (40 \pm 10)$ Å (Tien et al., 1966), $V = 0.1$ V, and averages of $\Delta\alpha_1/\alpha_1$ and $\Delta\alpha_3/\alpha_3$ over the four lowest dye concentrations in Figure 9 and Table I (where we assume only monomeric dye configurations to be significant; see below), we calculate $\mu = 8.6 \pm 2.3$ D. This value can be compared (favorably) with 9.70 ± 0.13 D obtained for a merocyanine with an identical chromophoric region by Kushner and Smyth (1949) (compare their structure II).

On the other hand, molecular reorientation alone is not sufficient to account for the dependence of the polarized flu-

orescence signals on dye concentration. There is good evidence from previous absorption experiments on axons for the presence of a nonfluorescent dimer species (Ross et al., 1974a,b; Warashina and Tasaki, 1975; Tasaki et al., 1976; Waggoner and Grinvald, 1977). Tasaki and Warashina (1976) and Warashina and Tasaki (1975) have also shown that the spectrum of absorption changes in axons is consistent with a combination of orientation change and spectral shift during depolarization and, if dimers are indeed present, that their absorption dipoles are aligned preferentially parallel to the membrane's surface. From the molecular structure in Figure 1 it appears that, if a dimer is formed by stacking two molecules together with molecular axes (and absorption dipoles) antiparallel, the electrostatic interaction energy between charges on the molecules will be minimized. It has been suggested that the cyanine dye methylene blue dimerizes in such a fashion (Förster, 1946; Bergmann and O'Konski, 1963). Since, as previously noted, it is also probable that the charged SO_3^- groups will remain at the aqueous interface, this dimer configuration would indeed be constrained to lie in the plane of the membrane.

A reexamination of the fluorescence response data of Figure 9 suggests a consolidated mechanism that accounts for these two bodies of evidence. As the M-540 concentration increases, it is seen that the polarized fluorescence responses originating from dye molecules oriented parallel to the membrane plane (Δ_{11}^f and Δ_{12}^f) undergo much more drastic changes (decreasing to nearly zero) than the responses originating from orientations normal to the membrane plane (Δ_{33}^f), which only increase slightly. (The trends in Δ_{13}^f and Δ_{31}^f are not convenient to analyze, since they are sensitive to contributions from both of the two symmetry directions.) If a large fraction of dye molecules oriented approximately parallel to the membrane plane is combined in the nonfluorescent dimer configuration, any change in the number of parallel monomers (e.g., by conversion to a more perpendicular orientation) would perturb the parallel monomer-dimer equilibrium, producing an opposite change in the number of dimers (i.e., the dimer concentration would decrease slightly to form more parallel monomers). In this way, a large dimer concentration could act as a buffer against voltage-induced changes in parallel monomer concentrations.

It remains to be seen whether dimer formation can quantitatively account for the concentration dependence of the fluorescence-polarization data. For this purpose, we next present a model calculation.

Quantitative Model of the Fast Fluorescence Response. We have developed some simple quantitative models for the fluorescence response based on the proposed mechanism of redistribution of molecular orientations by changes in membrane potential with an accompanying shift of monomer-dimer equilibrium. Their properties are calculated and compared with our experimental data in an attempt to appraise the indicated mechanism in greater detail. In these models, we assumed that the dye monomer appears on the membrane in only two discrete orientations: parallel to the surface of the membrane at concentration [A] or perpendicular to the membrane at concentration [B]. Even if the angular distribution of orientations is actually relatively uniform, this simplified model is sufficient to represent the fluorescence-polarization measurements, since all dipole orientations can be resolved into parallel and perpendicular components. Application of a membrane potential is assumed to alter the distribution between the two orientations.

Two additional features need to be included in the model: First, as required by previous discussion, a dimer species preferentially oriented parallel to the plane of the membrane at concentration $[A_2]$ is included. Second, saturation of the membrane with dye at high dye concentrations in solution is included by specifying a limited number of dye sites on the membrane. Saturation seems to be required to account for leveling off of the total membrane fluorescence and the decrease of the slow response Δ^s at high added dye concentrations (Figures 4 and 7).

In the absence of detailed information about dye binding sites on the membrane, various alternative models for saturation have been considered: (1) N sites per unit area for B type and N additional independent sites for A or A_2 types, with each A_2 occupying one site. (2) N sites per unit area for B type and N additional sites for A or A_2 types with each A_2 occupying two sites. (3) N sites accessible to A, B, or A_2 types with each A_2 occupying one site. (4) N sites accessible to A, B, or A_2 types with each A_2 occupying two sites. The first model is discussed fully as an illustration of the phenomena. The basic equations for the other three can be derived similarly, and the results will be discussed below. In analyzing the models, the variables are selected to display the results in terms of experimental observables. The densities of available sites N are unknown, and the dye activity on the membrane is not necessarily proportional to dye concentration in solution because the activity coefficient is affected by aggregate formation (Tasaki et al., 1976). Thus, the model calculations are derived as a function of the membrane concentrations [A] and [B], which will turn out to be proportional to experimental observables. For mass-action calculations, the thermodynamic activities a_A, a_{A_2}, and a_B for species A, B, and A_2 are defined. Saturation effects are incorporated by specifying corresponding activities a_α and a_β for vacant sites S_α (for type A or A_2) and vacant sites S_β (for type B), respectively.

For model (1) the relevant changes of state for dye binding on the membrane are

$$A + S_\beta \rightleftarrows B + S_\alpha \tag{4a}$$

$$2A \rightleftarrows A_2 + S_\alpha \tag{4b}$$

with corresponding equilibrium constants, respectively

$$K_0 \equiv \frac{a_B a_\alpha}{a_A a_\beta} = \frac{[B]}{[A]} \frac{N - [A] - [A_2]}{N - [B]} \tag{5a}$$

$$K_d \equiv \frac{a_{A_2} a_\alpha}{(a_A)^2} = \frac{[A_2](N - [A] - [A_2])}{[A]^2} \tag{5b}$$

Rearrangement yields the following expressions:

$$\frac{[A]}{[B]} = \{K_0 (1 - [B]/N) + [B]/N + [B]^2 K_d/[K_0 N(N - [B])]\}^{-1} \tag{6a}$$

$$[A_2] = 0.5(N - [A]) + 0.5[(N - [A])^2 - 4[A]^2 K_d]^{1/2} \times \begin{pmatrix} -1 \text{ for } [B] \le [B]_0 \\ +1 \text{ for } [B] > [B]_0 \end{pmatrix} \tag{6b}$$

where $[B]_0 \equiv N/(1 + K_d^{1/2}/K_0)$.

In the low dye concentration limit where $[A]/N \ll 1$ and $[B]/N \ll 1$, these results simplify to

$$[B]/[A] \simeq K_0$$

$$[A_2] \simeq K_d[A]^2/N \tag{7}$$

The concentration [B] will be regarded as the independent variable, since it is directly measured and proves to be convenient for comparison of model calculations with experiments.

To analyze the fast response to membrane potential changes

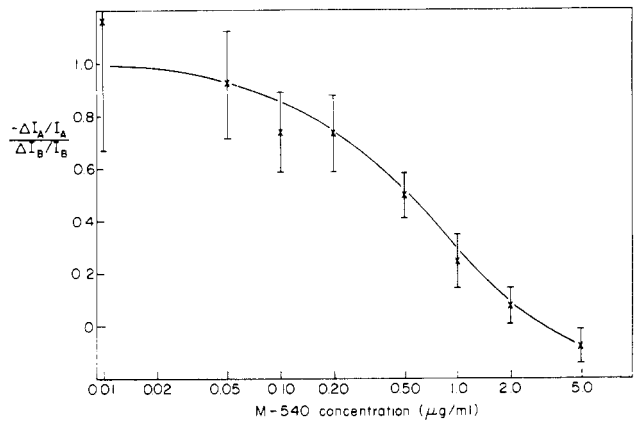

FIGURE 10: Relative magnitudes of parallel and perpendicular fast response $(-\Delta I_A/I_A)/(\Delta I_B/I_B)$ as a function of the M-540 concentration in the aqueous phase. $\Delta I_A/I_A = (\Sigma_j I_{1j}\Delta_{1j}^f)/\Sigma_i I_{1i}$ and $\Delta I_B/I_B = (\Sigma_j I_{3j}\Delta_{3j})/\Sigma_i I_{3i}$. The curve shown was drawn arbitrarily.

it is assumed that the sole effect of the membrane potential is to change the equilibrium constant K_0. The total dye concentration on the membrane is held constant during the fast response in order to comply with our experimental observation that the total dye concentration changes at least 10^5 times slower than the fast response considered here. Thus, we calculate the fractional changes $\Delta[A]$ and $\Delta[B]$ of the fluorescent parallel and perpendicular species A and B at constant total membrane-bound dye, i.e., with $[A] + [B] + 2[A_2] =$ constant.

$$\frac{\Delta[A]}{[A]} = \left(\frac{\partial \ln [A]}{\partial K_0}\right)' \Delta K_0$$

$$= \frac{-(N - [B])^2/N + [B]^2 K_d/(K_0^2 N)}{(N - [B])[B]/[A] + N - [A] + 4[A]K_d} \Delta K_0 \quad (8a)$$

$$\frac{\Delta[B]}{[B]} = \left(\frac{\partial \ln [B]}{\partial K_0}\right)' \Delta K_0$$

$$= -\frac{[A]}{[B]} \frac{(N - [A]) + 4[A]K_d}{[(N - [A])^2 - 4[A]^2 K_d]^{1/2}} \frac{\Delta[A]}{[A]}$$

$$\times \begin{pmatrix} 1 \text{ for } ([B] \leq [B]_0) \\ -1 \text{ for } ([B] > [B]_0) \end{pmatrix} \quad (8b)$$

where ΔK_0 is the change in K_0 caused by the change in membrane voltage and the prime denotes the condition $[A] + [B] + 2[A_2] =$ constant. In the low concentration limits, far from saturation ($[A]/N, [B]/N \ll 1$):

$$\frac{\Delta[A]}{[A]} \simeq \frac{-\Delta K_0}{1 + K_0 + 4K_d[A]/N} \quad (9a)$$

$$\frac{\Delta[B]}{[B]} \simeq \frac{\Delta K_0}{K_0} - \frac{\Delta K_0}{1 + K_0 + 4K_d[A]/N} \quad (9b)$$

In order to compare the fluorescence measurements with eq 6 and 8, it is necessary to determine [A] and [B] experimentally and estimate N, K_0, K_d, and ΔK_0. As will be shown shortly, K_0 and ΔK_0 can be determined using only the low concentration limit of the fluorescence response, and [A] and [B] can be calculated from the static fluorescence polarization measurements of Table I and the membrane FCS experiment described earlier. It will then remain to check that N and K_d can be chosen so that eq 6 and 8 fit both the static fluorescence and the fast fluorescence response data over the entire investigated concentration range.

Since only B-type molecules are excited by light polarized in the 3 direction, the fluorescence from B is given by $I_B = (I_{31} + I_{32} + I_{33}) = \alpha_3$. Similarly, the fluorescence from A-type molecules is $I_A = 2(I_{11} + I_{12} + I_{13}) = 2\alpha_1$; the factor of 2 is necessary because only half the A-type molecules are excited by 1-polarized light. I_A and I_B are related to A and B by

$$I_A = Q_A[A]$$

$$I_B = Q_B[B] \quad (10)$$

where the proportionality constants Q include quantum efficiencies and absorption coefficients. If the quantum efficiencies and absorption coefficients are independent of molecular orientation, $Q_A = Q_B$. However, given the facts that M-540 is very sensitive to the polarity of its surroundings and that the dielectric constant and index of refraction are nonisotropic in membranes (Ohki, 1968; Tasaki et al., 1976), this assumption may be unwarranted. Note, however, that the measurable parameters $\Delta I_A/I_A = \Delta[A]/[A]$ and $\Delta I_B/I_B = \Delta[B]/[B]$ are independent of Q_A and Q_B.

At low concentrations where saturation and dimerization effects are negligible, the limiting forms of eq 6 and 8 simplify sufficiently that the equilibrium constant K_0, the change in K_0 with voltage (ΔK_0), and the ratio of quantum efficiencies Q_A/Q_B can be determined directly from our experiment. In this limit, $\Delta[A] = -\Delta[B]$ and $(\Delta I_A/I_A)/(\Delta I_B/I_B) = (\Delta[A]/[A])/(\Delta[B]/[B]) = -[B]/[A] = -K_0$. Values of $(\Delta I_A/I_A)$ and $(\Delta I_B/I_B)$ can be calculated from the measurements of Δ_{ij}^f and I_{ij}. Extrapolating $(-\Delta I_A/I_A)/(\Delta I_B/I_B)$ to low concentrations (Figure 10) shows $K_0 \simeq 1.0$. Using this value with eq 9 and 10, we obtain $I_A/I_B = K_0 Q_A/Q_B = 2.4 \pm 0.4$ and $\Delta I_B/I_B - \Delta I_A/I_A = \Delta K_0/K_0 = 0.090 \pm 0.011$. These values are averages plus or minus the standard deviations of the values calculated from the data at M-540 solution concentrations in the range 0.01–0.2 μg/mL; here we assume that the corresponding dye concentrations on the membrane satisfy the low concentration limits. From these values we calculate $\Delta K_0 = 0.090 \pm 0.014$ and $Q_A/Q_B = 2.4 \pm 0.4$.

Q_A and Q_B can be calculated using the membrane dye concentration measured in the FCS experiment. Figure 4 shows that the total membrane fluorescence is approximately linearly proportional to the concentration of M-540 in the aqueous phase at low concentrations. With this assumption, Figure 4 can be used to estimate the total membrane fluorescence at the particular dye concentration determined in the FCS experiment. Defining this fluorescence photocurrent as I_0, and the corresponding membrane dye concentration $[X]_0$, Q_A and Q_B can be calculated as follows. Using eq 7 and 10 and the fact that $[X]_0 = [A] + [B]$ (since the dimer concentration is assumed negligible at this low concentration), we obtain

$$[A] = [X]_0/(1 + K_0) \quad (11)$$

and

$$I_0 = Q_A[A] + Q_B([X]_0 - [A]) \quad (12)$$

from which

$$Q_B = \frac{I_0(1 + K_0)}{(Q_A/Q_B + K_0)[X]_0} \quad (13)$$

Using $I_0 = 3.4 \times 10^{-9}$ A (Figure 4 at 0.01 μg/mL M-540 concentration) and the FCS experimental value of $[X]_0 = 3.54 \times 10^9$ molecules/cm^2, eq 13 gives $Q_B = (5.7 \pm 1.0) \times 10^{-19}$ A cm^2/molecule, and a similar calculation yields $Q_A = (1.4 \pm 0.2) \times 10^{-18}$ A cm^2/molecule. These proportionality constants allow the calculation of the important parallel and perpendicular components [A] and [B] at all M-540 solution concentrations, as shown in Figure 11. This figure also shows the values of $\Delta[A]/[A]$ and $\Delta[B]/[B]$ calculated directly from the fluorescence data of Figure 9 and Table I. Note that the

calculation of [A] and [B] uses the static fluorescence data of Table I, with the values of Q_A and Q_B determined as above using the model calculation in the low concentration limit. Values of $\Delta[A]/[A]$ and $\Delta[B]/[B]$ are calculable from Table I and Figure 9 directly as

$$\sum_{j=1}^{3} (\Delta_{1j}{}^{f}I_{ij}) / \sum_{j=1}^{3} I_{1j}$$

and

$$\sum_{j=1}^{3} (\Delta_{3j}{}^{f}I_{3j}) / \sum_{j=1}^{3} I_{3j}$$

respectively, and thus are model independent. The data in Figure 11 are displayed as a function of [B] for ease in comparison with the theoretical calculations of eq 6 and 8, as explained above.

Having thus deduced Q_A, Q_B, K_0, and ΔK_0 from the fluorescence data in the low concentration limit, the theoretical expressions for [A], $\Delta[A]/[A]$, and $\Delta[B]/[B]$ (eq 6 and 8) can be fitted to the fluorescence data by adjusting the parameters K_d and N. The results of the model calculations are compared with the directly measured fluorescence results in Figure 11. The decrease in $\Delta[A]/[A]$ toward zero at high dye concentrations is due to the "buffering" action of the presence of a large dimer concentration, as explained above. For example, if [A] were decreased slightly by a potential change that causes conversion to B, the equilibrium between A and A_2 would be perturbed such that a net dimer dissociation would occur, creating more fluorescent A. Changes in A are thereby resisted at high A_2 concentrations. At the highest concentration used, it appears that approximately 45% of the parallel sites and 25% of the perpendicular sites are occupied in this model.

The major features of our fluorescence-polarization data are reproduced by the results of the model calculations shown in Figure 11: $\Delta[B]/[B]$ increases slightly with dye concentration, $\Delta[A]/[A]$ decreases in magnitude toward zero, and [A] tends to saturate at high dye concentrations. Thus, the model calculations tend to support our major hypotheses of a mechanism with membrane potential induced molecular reorientation with an accompanying shift in monomer–dimer equilibrium. Minor disparities between the model calculations and data do exist, however (e.g., Figure 11a at high concentration), but because of many simplifications in the model we do not consider them significant in deciding the validity of our hypothesized model. In particular, we have assumed the A_2 species to exist in the parallel orientation only and that its fluorescence is negligible. (Evidence from axon absorption measurements concerning the dimer orientation will be discussed below.) Waggoner and Grinvald (1977) have also reported observing low fluorescence levels associated with M-540 dimers. We have also neglected effects of alternative secondary processes that, while not primarily responsible for the observed fluorescence changes, may nonetheless produce detectable effects on the fluorescence signals. For example, at the highest dye concentrations it is conceivable that resonant fluorescence energy transfer could occur. The fluorescence depolarization effect that this would produce would not be noticeable in the data of Figure 11, since, for each orientation of the excitation polarization, all emission polarizations are summed. A decrease in fluorescence quantum efficiency at high dye concentrations due to self quenching or energy transfer from A to A_2 type molecules[3] would, however, lead to an underestimation of the

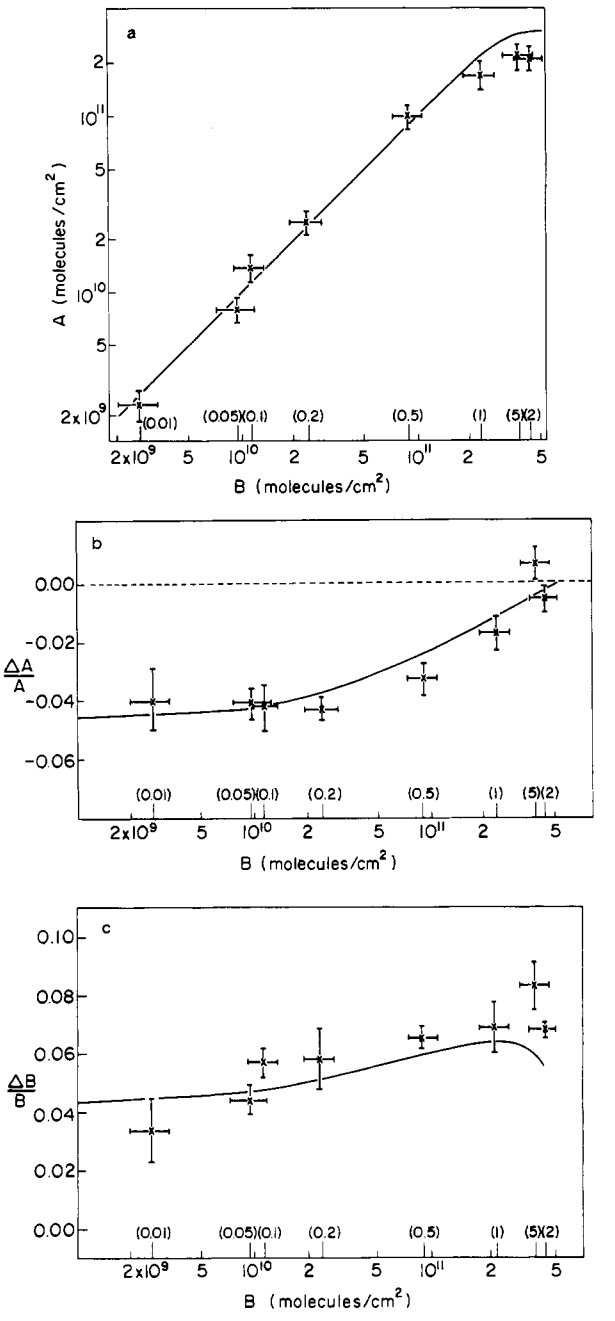

FIGURE 11: Comparison of theoretical model with experimental results: (a) Concentration of A, (b) $\Delta[A]/[A]$, (c) $\Delta[B]/[B]$, all are shown as a function of [B], calculated as $(1/Q_B)\Sigma_{j=1}^{3} I_{3j}$. The corresponding aqueous solution concentrations of M-540 (in μg/mL) are shown just above the abscissa. The experimental points are calculated from the data of Table I and Figure 9, and the solid curves are from the theory of eq 6 and 8. All error bars are derived from the standard deviations of the fluorescence measurements. Horizontal error bars are uncertainties in B: $K_0 = 1.0$, $\Delta K_0 = 0.090$, $N = 2 \times 10^{12}$ sites/cm^2, and $K_d = 8$.

A concentration. Correction for this effect would improve the agreement between theory and experiment in Figure 11a. It is also assumed in model (1) that there are discrete membrane sites for the dye of two types, one for B-type and the other for A- and A_2-type species, and that the densities of these sites are equal. An A_2 dimer will probably occupy more membrane area than one A-type monomer but less than two monomers. Therefore, modeling the effects of membrane saturation by assigning just one site per dimer is certainly an oversimplification. Similarly, the assumption of equal numbers of independent A and B type sites can only approximate the real sit-

[3] A second peak in the dimer absorption spectrum has recently been observed. Its overlap with the monomer emission peak is sufficient to make monomer to dimer resonant energy transfer plausible (Waggoner and Grinvald, 1977).

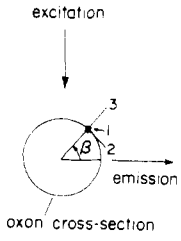

weight from		$I_{\parallel,\parallel}$	$I_{\parallel,\perp}$	$I_{\perp,\parallel}$	$I_{\perp,\perp}$
excitation	1	1	1	0	0
polarization	2	0	0	$\sin^2\beta$	$\sin^2\beta$
direction	3	0	0	$\cos^2\beta$	$\cos^2\beta$
emission	1	1	0	1	0
polarization	2	0	$\cos^2\beta$	0	$\cos^2\beta$
direction	3	0	$\sin^2\beta$	0	$\sin^2\beta$

FIGURE 12: Geometry and weighting factors for calculation of fluorescence changes in a cylindrical (axonlike) geometry from the measured I_{ij} and $\Delta_{ij}{}^{f}$. A cross section of the axon is shown, along with excitation and emission directions and the coordinate axes at a point on the membrane denoted by the angle β. The weighting factors at this point for the I_{ij} which contribute to the four fluorescence polarization intensities are given in the table.

uation. The distinct configuration visualized for these two types of sites suggests their independence. However, equality of number density was postulated merely to limit the number of adjustable parameters in the model.

We have investigated the effects of some of the above assumptions by examining the alternative models (1-4). If A_2 dimers are allowed to occupy two membrane sites (model 2), the experimental data can be fitted nearly as well as with model (1). However, if we assume only one type of membrane binding site, then $[A] = [B]/K_0$ independently of the total amount of dye on the membrane. Since this is not the observed result (Figure 11a), two site types seem to be required. However, selective quenching of the fluorescence of A type monomers at high concentration could be involved in the nonlinearity seen in Figure 11a. If this effect were present, the alternative models 3 and 4 could be made to fit the data in Figures 11b and 11c quite well.

Models 1 and 3, which postulate one site for each dimer, also predict that $\Delta[A]/[A]$ will cross zero and become positive at very high dye concentrations, whereas in models 2 and 4 $\Delta[A]/[A]$ does not change sign. We have, in fact, observed a positive value for $\Delta[A]/[A]$ at the highest dye concentration used (5 μg/mL, Figure 11b). However, the directly measured quantities $\Delta_{11}{}^{f}$ and $\Delta_{12}{}^{f}$, which are sensitive only to parallel monomers (A type), generally remain negative at all dye concentrations (Figure 9), although positive values were rarely observed in a few individual measurements. Therefore, in the absence of measurements at much higher M-540 concentrations, we cannot discriminate confidently between these alternative details of the saturation effects. Nevertheless, the basic molecular reorientation mechanism responsible for the polarized fluorescence response to fast membrane-potential changes is insensitive to these details.

The basic mechanism presented here is also consistent with absorption changes that have previously been observed in nerve axons stained with merocyanine M-540. A positive voltage pulse (corresponding to a depolarization of externally labelled axons) is predicted by our mechanism to decrease the membrane concentration of dimers at high dye concentrations. Since the absorption maxima of the monomer and dimer species occur at approximately 570 and 510 nm, respectively, this effect would produce an absorption decrease at short wavelengths and an increase at longer wavelengths; this is precisely what has been observed (Ross et al., 1974a,b; Tasaki et al., 1976). These results do substantiate the monomer–dimer equilibrium effect. The signs of the fast fluorescence responses are likewise consistent with predictions based on the reorientation model (see following section).

Application to Nerve Axons. In this section, we calculate the fluorescence intensities in an axonlike geometry in terms of our polarized fluorescence intensities defined under Results and Discussion section on fluorescence polarization notation, and show that our data account for observed fluorescence signals in axons. We will also compare absorption measurements on axons with predictions from our model.

The data presented in Table I and Figure 9 can be used to predict fluorescence intensity changes for measurements on a cylindrical membrane, the geometry of optical experiments on axons. Figure 12 shows the weighting factors for the various excitation and emission polarizations as a function of the position on the axon membrane denoted by the angle β. With the proper weights, the fluorescence intensities are calculated by averaging over $0 \le \beta \le \pi$. For example, $I_{\parallel,\perp}$, the fluorescence intensity with excitation polarization parallel to the axis of the axon and emission polarization perpendicular to the axis, is given by

$$I_{\parallel,\perp} = \frac{1}{2\pi}\int_0^{2\pi} d\beta(I_{12}\cos^2\beta + I_{13}\sin^2\beta) = \frac{1}{2}(I_{12} + I_{13})$$

Similarly,

$$\begin{aligned} I_{\parallel,\parallel} &= I_{11} \\ I_{\perp,\parallel} &= \frac{1}{2}(I_{21} + I_{31}) \\ I_{\perp,\perp} &= \frac{1}{8}(I_{33} + I_{11} + 3I_{31} + 3I_{13}) \\ I_{up} &= \frac{9}{8}I_{11} + \frac{1}{8}I_{33} + I_{12} + \frac{7}{8}I_{31} + \frac{7}{8}I_{13} \end{aligned} \tag{14}$$

I_{up} is the result if the excitation light is unpolarized. From these expressions, the fast fractional fluorescence changes for an axon can be calculated from our measured values of I_{ij} and $\Delta_{ij}{}^{f}$; the results are presented in Table II. Here Δ^{c} refers to fast fluorescence changes in a cylindrical membrane geometry. Notice that both the magnitude and sign of the effect change with polarization and dye concentration.

The sign of the fluorescence response in the unpolarized case at the highest concentration in Table II agrees with that observed in experiments on axons (Davila et al., 1973), but the predicted magnitude is larger by about ten times. This difference is to be expected, since in tissue most of the dye binds to membranes other than the active axon membrane in the squid giant axon. Cohen et al. (1974) estimated the axon-membrane associated fluorescence change to be 1% at least. All reported experiments on axons stained with M-540 have used relatively high dye concentrations; thus, the predicted reversal of sign of the response at low dye concentrations has not yet been observed on nerve. It is also interesting to note that the signal level in $\Delta_{up}{}^{c}$ is most favorable at high dye concentrations for two distinct reasons: the overall fluorescence intensity is higher, and contributions of negative sign ($\Delta_{11}{}^{f}$ and $\Delta_{12}{}^{f}$) are suppressed. Hence, the decrease in $\Delta_{11}{}^{f}$ and $\Delta_{12}{}^{f}$, which our model attributes to the "buffering" action of the dimer species, enhances the fluorescence changes seen with M-540 in axons.

Warashina and Tasaki (1975) have separated the contributions of the monomer and dimer species to polarized absorption signals during action potentials in axons. They estimated the ratio of the dimer absorption change with light polarized normal to the axon axis to that with light polarized parallel to the axis to be 0.74. Assuming that the dimers are oriented either parallel or perpendicular to the membrane

TABLE II: Fluorescence Response Calculated for Axonlike Geometry.[a]

M-540 concn (μg/mL)	$\Delta_{\parallel,\parallel}$[c]	$\Delta_{\parallel,\perp}$[c]	$\Delta_{\perp,\parallel}$[c]	$\Delta_{\perp,\perp}$[c]	Δ_{up}[c]
5	−0.014 (±0.008)	0.023 (±0.007)	0.027 (±0.006)	0.057 (±0.005)	0.022 (±0.005)
2	−0.034 (±0.007)	0.013 (±0.005)	0.023 (±0.005)	0.047 (±0.002)	0.013 (±0.003)
1	−0.046 (±0.008)	0.002 (±0.007)	−0.004 (±0.009)	0.037 (±0.005)	−0.005 (±0.006)
0.5	−0.052 (±0.009)	−0.016 (±0.006)	−0.029 (±0.007)	0.019 (±0.004)	−0.024 (±0.005)
0.2	−0.063 (±0.005)	−0.017 (±0.004)	−0.030 (±0.006)	0.010 (±0.004)	−0.033 (±0.004)
0.1	−0.068 (±0.016)	−0.019 (±0.006)	−0.032 (±0.007)	0.008 (±0.005)	−0.034 (±0.008)
0.05	−0.051 (±0.008)	−0.026 (±0.004)	−0.024 (±0.008)	0.008 (±0.007)	−0.029 (±0.005)
0.01	−0.045 (±0.011)	−0.031 (±0.020)	−0.031 (±0.021)	0.002 (±0.012)	−0.030 (±0.009)

[a] Uncertainty values are from standard deviations of the fluorescence measurements. Units are per 100-mV membrane potential change, inside positive (depolarization), with the dye applied to the outside.

surface and that this ratio is equal to the ratio of the static absorbances, then it can be shown that

$$0.74 = \left(\frac{1}{2}C_{\parallel}^{d} + C_{\perp}^{d}\right)/C_{\parallel}^{d}$$

where $C_{\parallel}^{d}$ and $C_{\perp}^{d}$ are the concentrations of parallel- and perpendicular-oriented dimers, respectively. Thus, $C_{\perp}^{d}/C_{\parallel}^{d} = 0.24$, or 81% of the dimers have the parallel orientation. To the extent that the above assumptions are valid, this supports the postulated parallel dimer orientation in our model.

Despite the consistency displayed above, direct quantitative comparison between results from our model membrane system and measurements on nerve axons should be approached with caution for the following reasons: (1) Experiments on nerve have usually employed higher dye concentrations than our studies (often with detergent present to solubilize the dye). (2) Our membranes were formed in 0.1 M salt, while squid axon experiments use salt concentrations five times higher. Waggoner and Grinvald observed that the solubility of the dye in aqueous solution decreases with increasing salt concentrations and that the amount of M-540 dimers detected on phosphatidylcholine vesicles increased significantly at the higher salt concentration (A. Grinvald, personal communication). Easton et al. (1978) have also recently observed that uptake of dye by electrically excitable cells depends on ionic strength and on multivalent cations, although they did not distinguish between dye transport into the cell and surface staining of the plasma membrane. (3) Polarized absorption measurements in externally stained crab nerve and squid axons have shown that action potentials are accompanied not only by the predicted decrease in dimer absorption (~460–550 nm) but also by an increase in absorption by parallel-oriented monomer (~550–600 nm). This bimodal response has not been seen with internally stained squid axons, however, which showed a spectral dependence consistent with a change only in parallel-oriented dimers (Warashina and Tasaki, 1975; Tasaki and Warashina, 1976; Ross et al., 1977). Our results are consistent with these observations in the dimer band but predict a decrease in absorbance in the monomer band at low dye concentration and no change ($\Delta[A]/[A] \rightarrow 0$, Figure 11b) at our highest dye concentrations. However, as mentioned above under the Results and Discussion section on the quantitative model of the fast fluorescence response, extrapolating some of our model calculations to yet higher dye concentrations predicts an increase in the number of parallel-oriented monomers; our experimental observations support this trend. This extrapolation predicts absorption signals consistent with the observations of Tasaki and Warashina (1976) and Ross et al. (1977).

Despite the fact that our measurements were performed on a model membrane system under somewhat different conditions than nerve experiments, we nevertheless think that the mechanism we have found applies also in the nerve experiments and that the apparent discrepancies are due to differences in dye concentrations in the membranes.

Summary

Our experiments suggest mechanisms for both slow and fast responses of M-540 to membrane potential.

Voltage-induced changes in the membrane dye concentration are responsible for the slow response. There was no noticeable dependence on the polarization of the observed fluorescence, the response decreased at high dye concentrations where the membrane dye concentration saturated, and the sign of the molecular charge was consistent with the observed sign of the fluorescent changes. Furthermore, the observed time constant of the fluorescence response agreed with the theoretical analysis of this kind of mechanism worked out by Conti et al. (1974).

The fast fluorescence response, on the other hand, is based on a change in the distribution of molecular orientations of M-540 in response to an applied electric field. Evidence for M-540 reorientation was first presented by Warashina and Tasaki (1975) and Tasaki and Warashina (1976), who showed that the spectrum of absorption signals in axons is consistent with a combination spectral shift and molecular reorientation. We observed fast polarized fluorescence signals of opposite signs, depending on polarization, precisely as expected of molecular reorientation changes in the applied electric fields. As expected, the size of the fractional fluorescence response was independent of excitation or emission wavelength, and the rise time of the fluorescence changes was very fast (rise times less than 6 μs).

Components of fluorescence responses due to dye molecules

oriented parallel to the membrane surface saturated at high dye concentrations due to the formation of a nonfluorescent dimer oriented parallel to the membrane surface. The presence of nonfluorescent M-540 dimers has previously been inferred from absorption measurements in axons (Ross et al., 1974a,b; Warashina and Tasaki, 1975).

The major features of the observed fast fluorescence responses were reproduced by a model in which applied membrane voltages perturbed the equilibrium between two distinct groups of fluorescent monomers, one oriented parallel to the membrane surface and the other group perpendicular. Dimerization of the parallel monomers, with the dimer nonfluorescent, accounts for the fluorescence saturation at high dye concentrations if a finite number of dye binding sites were postulated for both parallel and perpendicular species. The agreement between this model and the fluorescence measurements is illustrated in Figure 11.

Acknowledgments

We are pleased to acknowledge that we were stimulated by Dr. Paul Mueller to carry out this type of experiment and that we had the help of informative conversations with Drs. Lawrence Cohen, Amirim Grinvald, and Alan Waggoner. We also thank Drs. Grinvald, Ichiji Tasaki, and John Weinstein for reviewing the manuscript and Mrs. Helen Bell and Mrs. Barbara Meger for typographical service.

References

Badley, R. A., Schneider, H., and Martin, W. G. (1971), *Biochem. Biophys. Res. Commun. 45,* 174.

Badley, R. A., Schneider, H., and Martin, W. G. (1972), *Biochem. Biophys. Res. Commun. 49,* 1292.

Badley, R. A., Martin, W. G., and Schneider, M. (1973), *Biochemistry 12,* 268.

Bergmann, K., and O'Konski, C. T. (1963), *J. Phys. Chem. 67,* 2169.

Brooker, L. G. S., Cragi, A. C., Haseltine, D. W., Jenkins, P. W., and Lincoln, L. L. (1965), *J. Am. Chem. Soc. 87,* 2443.

Bücher, H., Wiegand, J., Snavely, B. B., Beck, K. H., and Kuhn, H. (1969), *Chem. Phys. Lett. 3,* 508.

Carbone, E., Conti, F., and Fioravanti, R. (1975), *Biophys. Struct. Mech. 1,* 221.

Carney, L. D., and Barry, W. H. (1969), *Science 165,* 608.

Cogan, U., Shinitzky, M., Weber, G., and Nishida, T. (1973), *Biochemistry 12,* 521.

Cohen, L. B., Salzberg, B. M., Davila, H. V., Ross, W. N., Landowne, D., Waggoner, A. S., and Wang, C. H. (1974), *J. Membr. Biol. 19,* 1.

Conti, F., Fioravanti, R., Malerba, F., and Wanke, E. (1974), *Biophys. Struct. Mech. 1,* 27.

Davila, H. V., Salzberg, B. M., Cohen, L. B., and Waggoner, A. S. (1973), *Nature (London), New Biol. 241,* 159.

Dragsten, P. R. (1977), Ph.D. Thesis, Cornell University.

Dragsten, P. R., and Webb, W. W. (1977), *Biophys. J. 17,* 215a.

Elson, E. L., and Magde, D. (1974), *Biopolymers 13,* 1.

Fahey, P. F., Koppel, D. E., Barak, L. S., Wolf, D. E., Elson, E. L., and Webb, W. W. (1976), *Science 195,* 305.

Förster, T. (1946), *Naturwissenschaften 33,* 166.

Frehland, E., and Trissl, H. W. (1975), *J. Membr. Biol. 21,* 147.

Koppel, D. E., Axelrod, D., Schlessinger, J., Elson, E. L., and Webb, W. W. (1976), *Biophys. J. 16,* 1315.

Kushner, L. M., and Smyth, C. P. (1949), *J. Am. Chem. Soc. 71,* 1401.

Landowne, D. (1974), *J. Gen. Physiol. 64,* 5a.

Liptay, W. (1969), *Angew. Chem., Int. Ed. Engl. 8,* 177.

Magde, D., Elson, E. L., and Webb, W. W. (1972), *Phys. Rev. Lett. 29,* 705.

Magde, D., Elson, E. L., and Webb, W. W. (1974), *Biopolymers 13,* 29.

Oetliker, H., Baylor, S. M., and Chandler, W. K. (1975), *Nature (London) 257,* 693.

Platt, J. R. (1969), *J. Chem. Phys. 34,* 862.

Ross, W. N., Salzberg, B. M., Cohen, L. B., and Davila, H. V. (1974a), *Biophys. J. 14,* 983.

Ross, W. N., Salzberg, B. M., Cohen, L. B., Davila, H. V., Waggoner, A. S., and Wang, C. H. (1974b), *Biol. Bull. (Woods Hole, Mass.) 147,* 496.

Ross, W. N., Salzberg, B. M., Cohen, L. B., Grinvald, A., Davila, H. B., Waggoner, A. S., and Wang, C. H. (1977), *J. Membr. Biol. 33,* 141.

Salama, G., and Morad, M. (1976), *Science 191,* 485.

Salzberg, B. M., Davila, H. V., and Cohen, L. B. (1973), *Nature (London) 246,* 508.

Shinitzky, M., and Inbar, M. (1976), *Biochim. Biophys. Acta 433,* 133.

Sims, P. J., Waggoner, A. S., Wang, C. H., and Hoffman, J. F. (1974), *Biochemistry 13,* 3315.

Tanford, C. (1961), New York, N.Y., Wiley, p 436.

Tasaki, I., and Warashina, A. (1976), *Photochem. Photobiol. 24,* 191.

Tasaki, I., Watanabe, A., Sandlin, R., and Carnay, L. (1968), *Proc. Natl. Acad. Sci. U.S.A. 61,* 883.

Tasaki, I., Hallett, M., and Carbone, E. (1973), *J. Membr. Biol. 11,* 353.

Tien, H. T. (1974), New York, N.Y., Marcel Dekker, p 483.

Tien, H. T., Carbone, S., and Dawidowicz, E. A. (1966), *Nature (London) 212,* 718.

Vergara, J., and Bezanilla, F. (1976), *Nature (London) 259,* 684.

Waggoner, A. (1976), *J. Membr. Biol. 27,* 317.

Waggoner, A. S., and Grinvald, A. (1977), *Ann. N.Y. Acad. Sci. 303,* 217.

Warashina, A., and Tasaki, I. (1975), *Proc. Jpn. Acad. 51,* 610.

West, W., and Pearce, S. (1965), *J. Phys. Chem. 69,* 1894.

Yguerabide, L., and Stryer, L. (1971), *Proc. Natl. Acad. Sci. U.S.A. 68,* 1217.